

# Adversarial Multi-Agent Reinforcement Learning for Proactive False Data Injection Detection

Kejun Chen<sup>†</sup>, Truc Nguyen<sup>†</sup>, Malik Hassanaly<sup>†</sup>

**Abstract**—Smart inverters are instrumental in the integration of renewable and distributed energy resources (DERs) into the electric grid. Such inverters rely on communication layers for continuous control and monitoring, potentially exposing them to cyber-physical attacks such as false data injection attacks (FDIAs). We propose to construct a defense strategy against a priori unknown FDIAs with a multi-agent reinforcement learning (MARL) framework. The first agent is an adversary that simulates and discovers various FDIA strategies, while the second agent is a defender in charge of detecting and localizing FDIAs. This approach enables the defender to be trained against new FDIAs continuously generated by the adversary. The numerical results demonstrate that the proposed MARL defender outperforms a supervised offline defender. Additionally, we show that the detection skills of an MARL defender can be combined with that of an offline defender through a transfer learning approach.

## I. INTRODUCTION

Integrating distributed energy resources (DERs) into an electric grid inherently reduces the grid’s inertia, making it less resilient to frequency instabilities [1]. Smart inverters are a promising solution that can help regulate voltage and frequency, thanks to actuation strategies that depend on the state of the system [2]. Smart inverters rely on information exchange, either through observations of the state of the grid or through actuation decisions sent via communication networks [3]. This makes them a target for cyber-physical attacks, and in particular false data injection attacks (FDIAs) that tamper with sensor measurements [4] or even the control logic of the inverter [5]. Cyber-physical attacks are becoming a tangible risk: five consequential attacks were reported in 2023 [6], and fifteen FDIAs have been noted over the past ten years [7].

To address the risk of FDIAs, research efforts have focused on constructing accurate detection methods. FDIA detection methods typically rely on the comparison of a reference state

(without FDIAs) and the actual observed state. This approach can take the form of a state predictor [8] or the construction of a state embedding [9]. Discrepancies between reference and observed states are then used to decide whether an FDIA has occurred. To realize this detection principle, a data-based approach would involve training a model that distinguishes between FDIA data and benign data. This often requires some level of supervised training where one assumes how FDIAs occur [10], [11]. If the decision boundary is imperfect, the FDIA detection may become vulnerable to impactful and stealthy adversarial examples.

Identifying the vulnerabilities of FDIA detection methods has been the object of several research efforts. Previously, constrained optimization [12], [13] and adversarial learning [14] strategies have been used to defeat bad data detection models. The same optimization problem can be formulated with reinforcement learning (RL), which can be used for arbitrarily complex systems while generating hitherto unseen FDIAs by interacting with an environment [15]. This approach has been used to improve detection methods in the context of frequency control [16] and state estimation problems [17], [18]. These previous works only utilized a single RL agent to serve as either adversary or defender but did not consider concurrent adversarial training.

By contrast, we propose a multi-agent reinforcement learning (MARL) framework for concurrently training an FDIA adversary and defender. One of the key challenges of MARL’s training is the non-stationary environment for the competitive agents. To address this, the learning environment and reward function are strategically designed to achieve the simultaneous performance improvement of both the adversary and defender agents. Even if the adversary continuously generates novel FDIAs to disrupt the system frequency, the defender can promptly adjust its behavior and update its defense strategy accordingly. The contribution of this paper is twofold:

- Without prior knowledge, we demonstrate how a defender trained with the proposed MARL framework can handle continuously varying unknown adversarial attacks launched by an adversary.
- We show that prior knowledge from an offline-trained defender can be retained through a transfer learning approach. Experiments show that this strategy enhances the performance of the MARL defender on unseen FDIAs during the MARL training procedure.

Sec. II formulates the FDIA detection problem. Sec. III describes the MARL framework and Sec. IV evaluates its performance. Finally, Sec. V concludes the manuscript.

<sup>†</sup>Computational Science Center, National Renewable Energy Laboratory (NREL), Golden, CO, USA. Emails: {kejun.chen, truc.nguyen, malik.hassanaly}@nrel.gov. The corresponding author is Kejun Chen.

We thank Dr. Abhijeet Sahu for the helpful discussions on the state prediction model, and Dr. Xiangyu Zhang for his early work on this topic. This work was authored by the National Renewable Energy Laboratory, operated by Alliance for Sustainable Energy, LLC, for the U.S. Department of Energy (DOE) under Contract No. DE-AC36-08GO28308. This work was supported by the Laboratory Directed Research and Development (LDRD) Program at NREL. The views expressed in the article do not necessarily represent the views of the DOE or the U.S. Government. The U.S. Government retains and the publisher, by accepting the article for publication, acknowledges that the U.S. Government retains a nonexclusive, paid-up, irrevocable, worldwide license to publish or reproduce the published form of this work, or allow others to do so, for U.S. Government purposes. This research was performed using computational resources sponsored by the DOE’s Office of Energy Efficiency and Renewable Energy and located at the NREL.

## II. PROBLEM FORMULATION

### A. Frequency Control in Power System

Consider a power grid with a set  $\mathcal{N}$  of  $N$  buses. The system state  $\mathbf{s} := [\boldsymbol{\theta}^\top; \boldsymbol{\omega}^\top]^\top \in \mathbb{R}^{2N}$  contains phase angles and frequency deviation of all buses. The primary frequency dynamics can be expressed as the swing equation [19]:

$$\dot{\theta}_i = \omega_i, \quad (1a)$$

$$M_i \dot{\omega}_i = p_i - p_i^{\text{IBR}}(\omega_i) - D_i \omega_i - \sum_{j=1}^N B_{ij} \sin(\theta_i - \theta_j), \quad (1b)$$

where  $M_i$  and  $D_i$  represent the inertia and damping coefficients of the  $i$ -th bus, respectively.  $p_i$  denotes the net power injection of bus  $i$  and  $B_{ij}$  is the  $(i, j)$ -th element in the susceptance matrix.  $p_i^{\text{IBR}}$  represents the active power output from the inverter-based resources (IBR) at bus  $i$ , which can be controlled by the linear droop controller, i.e.,  $p_i^{\text{IBR}} := k_i^{\text{ref}} \omega_i$ . The droop coefficients can be designed using conventional optimization methods to stabilize the primary frequency under a random off-equilibrium initial condition [19]. The power system is time-constrained and each episode consists of  $T$  timesteps spanning the time interval  $[0, t_f]$ .

### B. False data injection attack

An adversary is assumed to have remote access to all  $N$  smart inverters of the system. Its objective is to induce frequency instability by modifying the droop coefficient of each inverter. The adversary can change only one coefficient at a time.

In the absence of detection, the adversary aims to solve the following optimization problem [15]:

$$\max_{k'_{i,t}} \sum_{t \in \mathcal{T}} \sum_{i \in \mathcal{N}} |\omega_{i,t}| - |\omega_{i,t}^{\text{ref}}|, \quad (2a)$$

$$\text{s.t. Eq. (1),} \quad (2b)$$

$$p_{i,t}^{\text{IBR}} = k'_{i,t} \omega_{i,t}, \quad (2c)$$

$$\|\mathbf{k}^{\text{ref}} - \mathbf{k}'_t\|_0 \leq 1, \quad (2d)$$

where  $\omega_i^{\text{ref}}$  denotes the frequency deviation of bus  $i$  using the unaltered droop controller. The objective function (2a) indicates the adversary aims to tamper with the droop coefficient (denoted by  $k'_i$ ) to maximize frequency deviation in the control horizon  $\mathcal{T} := \{0, \dots, T-1\}$ . Eq. (2d) ensures that at most one droop coefficient can be modified by the adversary at any timestep, where  $\mathbf{k}'_t \in \mathbb{R}^N$  denotes the vector of (tampered) droop coefficients at time  $t$  and  $\mathbf{k}^{\text{ref}}$  are the unaltered droop coefficients of all buses.

### C. False data injection detection

The detection method considered uses a long short-term memory (LSTM) state predictor that was proposed in Ref. [8]. The LSTM predicts the reference state at time  $t$  based on the observed states over the past  $d-1$  timesteps, i.e.,  $[\mathbf{s}_{t-(d-1)}, \dots, \mathbf{s}_{t-1}] \mapsto \hat{\mathbf{s}}_t$ . The defender is a multiclass classifier that localizes the attacked bus index based on the state prediction error, i.e.,  $\mathbf{s}_t^e \mapsto g_t^d \in \{-1, 0, \dots, N-1\}$ , where

$\mathbf{s}_t^e := c_w(\mathbf{s}_t - \hat{\mathbf{s}}_t)$ , where  $c_w$  is a scaling coefficient and the class  $-1$  implies that no attack occurs. The architecture of the offline defender is schematically shown in Fig. 1. Although the detection is called periodically every  $d$  timesteps, it can detect FDIAs that occurred over the past  $d-1$  timesteps [8]. The ensemble of detection timesteps is denoted by  $\mathcal{T}_d$  and  $\text{card}(\mathcal{T}_d) = T/d$ .

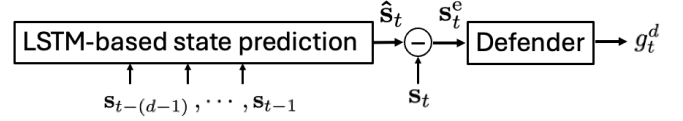


Fig. 1. Schematic of the offline FDIA defender.

To train the supervised classifier, one first synthetically constructs FDIAs, as described hereafter. At timestep  $t$ , if an FDIA occurs, the adversary modifies the droop coefficient of bus  $i$ . Otherwise, the unaltered droop coefficients are used. Throughout the episode, the training data is constructed by randomly selecting timesteps where an FDIA occurs. Let  $T_a$  denote the fraction of episode steps where an FDIA occurs and we have  $T_a \in \{0.16, 0.2, 0.4, 0.6, 0.8\}$  to simulate different adversarial scenarios (e.g.,  $T_a = 0.8$  implies an FDIA occurs for 80% of the episode). As shown in Fig. 2, the dataset comprises windows of length  $d$ . At most one bus is attacked per window, thereby alleviating any ambiguity about how each window is labeled. The offline defender will serve as a baseline for comparison with the MARL defender in Sec. IV.

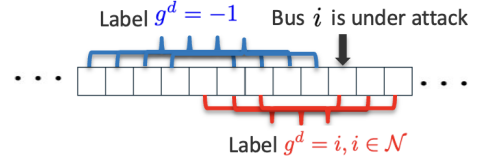


Fig. 2. The demonstration of defender's label under FDIAs at bus  $i$ .  $g^d$  denotes the attacked bus index identified by the defender (or  $-1$  if no attack).

## III. METHOD

Figure 3 illustrates the proposed MARL framework for proactive FDIA detection. The defender agent is a classifier that aims at detecting the bus under attack. The adversary agent seeks to disrupt the power grid frequency while avoiding being captured by the defender.

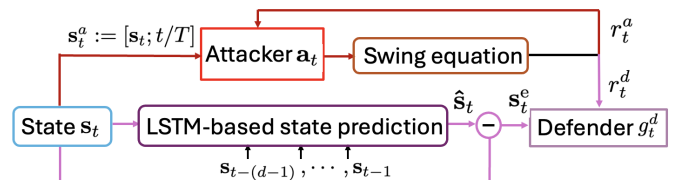


Fig. 3. Multi-agent framework for the FDIA detection.

### A. The proposed MARL framework.

1) *Adversary*: The adversary's observation space,  $\mathbf{s}_t^a$ , is the concatenation of the system state and the normalized simulation step, i.e.  $\mathbf{s}_t^a := [\boldsymbol{\theta}^\top, \boldsymbol{\omega}^\top, t/T]^\top$ . The normalized simulation step provides the current time to the adversary. The adversary's action space is  $\mathbf{a}_t = [g_t^A, c_t, m_t]$ , where  $g_t^A \in \{-1, 0, \dots, N-1\}$  represents the index of the bus attacked or  $-1$  for no attack,  $c_t$  is value with which the droop coefficient is replaced ( $k'_{i,t} = c_t$ ), and  $m_t$  is a boolean used to mute or not the attack. For simplification and consistency with refs. [8], [15],  $c_t \in \{-1, 0, 1\}$ . Given the detection time  $t \in \mathcal{T}_d$ , the detection window is defined as  $\mathcal{D}_t := [t - (d - 1), \dots, t]$ . We define  $g^a$  to record the attack bus index over  $\mathcal{D}_t$  and initialize it as  $-1$ . To mimic the synthetically generated FDIAs used for offline training, the following post-processing action mask mechanism is used to ensure that at most one bus is under attack over the detection window  $\mathcal{D}_t$ :

$$g_t^a = \begin{cases} g_t^A, & \text{if } g^a = -1, \\ g^a, & \text{if } m_t = 0 \wedge g^a \neq -1, \\ -1, & \text{if } m_t = 1 \wedge g^a \neq -1, \end{cases} \quad (3)$$

where,  $\wedge$  denotes the logical AND operator. Once the bus to attack is chosen with  $g_t^A$ , the binary variable  $m_t$  is used to decide whether to attack ( $m_t = 0$ ) or mute the attack ( $m_t = 1$ ). The stealthiness constraint is included in the new objective function Eq. (4) through a penalty  $p$  for being detected ( $p < 0$ ).

$$\max_{k'_i} \sum_{t \in \mathcal{T}} \left( (1 - D_t^{\text{suc}}) \sum_{i \in \mathcal{N}} (|\omega_i| - |\omega_i^{\text{ref}}|) + D_t^{\text{suc}} p \right), \quad (4a)$$

$$\text{s.t. Eq. (2b) - (2d),} \quad (4b)$$

$$D_t^{\text{suc}} = \begin{cases} 1, & \text{Captured by the defender at } t \in \mathcal{T}_d, \\ 0, & \text{Escape from detection at } t \in \mathcal{T}_d, \\ 0, & \text{Non-detection time } t \in \mathcal{T} \setminus \mathcal{T}_d. \end{cases} \quad (4c)$$

The instantaneous reward at time  $t$  is designed as:

$$r_t^a = \begin{cases} p, & g_t^a = g_t^d \wedge g_t^a \neq -1, t \in \mathcal{T}_d \\ r_t^\omega, & \text{otherwise,} \end{cases} \quad (5)$$

where  $r_t^\omega := c_s \sum_{i \in \mathcal{N}} (|\omega_{i,t}| - |\omega_{i,t}^{\text{ref}}|)$  represents the scaled frequency deviation difference compared to the default droop controller. A large reward value reflects that the adversary induced frequency instability, and that it escaped the defender. Hereafter, the adversary is referred to as MARL-A.

2) *Defender*: The defender agent is the multiclass classifier described in Sec. II-C. The LSTM is held frozen during the MARL training process. The defender's state space is  $\mathbf{s}_t$ . The action space  $g_t^d \in \{-1, 0, \dots, N-1\}$  represents the identified attacked bus index or  $-1$  for no attack. If the defender successfully identifies the attack status, it will receive a reward  $r > 0$  and a penalty  $-r$  otherwise. The instantaneous

---

### Algorithm 1 Multi-agent framework for FDIA detection.

---

```

1: for episode  $e = 1, 2, \dots, K$  do
2:   Reset the initial state  $\mathbf{s}_0$ .
3:   for simulation step  $t = 0, 1, \dots, T - 1$  do
4:     Obtain the attack status  $g_t^a$  based on Eq. (3) and
      $c_t$  from the adversary's policy network  $\mathcal{A}_\alpha(\mathbf{a}_t|\mathbf{s}_t)$ .
5:     Calculate  $\mathbf{s}_{t+1}$  using the swing equation and obtain
     the reward  $r_t^a = r_t^\omega$ .
6:     if  $t \in \mathcal{T}_d$  then
7:       Apply the defender's policy network  $\mathcal{D}_\theta(g_t^d|\mathbf{s}_t)$ 
       and obtain the detected bus index  $g_t^d$ .
8:       if  $g_t^d = g_t^a$  then
9:         The reward of the defender is  $r_t^d = r$ .
10:      else
11:        The penalty to the defender is  $r_t^d = -r$ .
12:      end if
13:      if  $g_t^d = g_t^a \wedge g_t^a \neq -1$  then
14:        The penalty to the adversary is  $r_t^a = p$ 
15:      end if
16:      Calculate the total reward of the adversary over
       the detection window  $R_t = \sum_{t \in \mathcal{D}_t} r_t^a$ .
17:    end if
18:  end for
19:  Update the parameters of the policy networks.
20: end for

```

---

reward at time  $t$  is defined in Eq. 6. The defender aims to maximize the cumulative reward  $\max_{g_t^d} \sum_{t \in \mathcal{T}} r_t^d$ .

$$r_t^d = \begin{cases} r, & g_t^a = g_t^d, t \in \mathcal{T}_d, \\ -r, & g_t^a \neq g_t^d, t \in \mathcal{T}_d, \\ 0, & t \in \mathcal{T} \setminus \mathcal{T}_d. \end{cases} \quad (6)$$

In the rest of the text, the defender is referred to as MARL-D.

The concurrent training procedure of the attacker and defender is described in Algorithm 1.

### B. Warm-up strategy for MARL defender

Ideally, the adversarial training of the defender refines an offline-trained one instead of training it from scratch. This way, expert knowledge can be distilled into the defender, and it can still be made robust to adversarial examples. To achieve this goal, we use the offline defender described in Sec. II-C to initialize the policy neural network of the MARL-D. The goal of this procedure is to improve the defense strategy of the MARL-D against new adversarial attacks, while retaining the prior knowledge of the offline-trained defender. In the remainder of the text, MARL-D refers to an agent trained from a random weight initialization, while a TF-MARL-D is a defender for which transfer learning is used, and TF-MARL-A denotes its corresponding adversary. Note that transfer learning is only applied to the defender; MARL-A and TF-MARL-A always use a random weight initialization.

## IV. NUMERICAL RESULTS

### A. Simulation setup

The proposed framework is tested on the 10-bus Kron reduced IEEE New England 39-bus system, for which unaltered droop coefficients are provided in [19]. Here,  $t_f = 5\text{s}$ , and the simulation interval is  $0.01\text{s}$  leading to a total number of steps per episode  $T = 500$ . Consistently with Ref. [8], the window length is set to  $d = 6$  and the ensemble of detection timesteps is therefore  $\mathcal{T}_d := \{6, 12, \dots, 498\}$ . Initial conditions are constructed by superimposing disturbances onto the equilibrium state. Disturbances are sampled from  $\mathcal{U}(-0.2, 0.2)$  for both the phase and frequency. The same initial condition is used in MARL and offline defender training. In the adversary reward (Eq. 4c),  $c_s = 0.1$  to avoid large training reward values and stabilize the training process. The reward for a successful defense and the penalty for being captured are given as  $r = -p = 0.1$ , and  $c_w$  is set to 100. We use the Ray library with TensorFlow to train MARL using the proximal policy optimization (PPO) algorithm [20], where the entropy coefficient and the clip range are set to 0.01 and 0.2, respectively. The LSTM is the same as the one described in ref. [8] and uses 100 units. The policy neural networks of the adversary and defender contain two hidden layers, each consisting of 256 neurons with a hyperbolic tangent (tanh) activation function. The train-batch and mini-batch sizes are set to  $10^5$  and 128, respectively. The learning rate is set to  $10^{-4}$ , and the rollout fragment length is set to 500. We implement the simulations using the high performance computing (HPC) system in parallel across multiple nodes with multiple CPU cores.

### B. MARL detection vs offline-trained defender

Figure 4 illustrates the training rewards under 5 independent simulation runs. In the following figures, only the results of the training run that leads to the highest accuracy for the MARL-D are shown. As shown in Fig. 5a, the adversary typically chooses  $c_t = -1$  because a negative value of  $c_t$  leads to more impactful attacks [15]. Figure 5b shows the resulting frequency instability of each bus caused by the MARL-A.

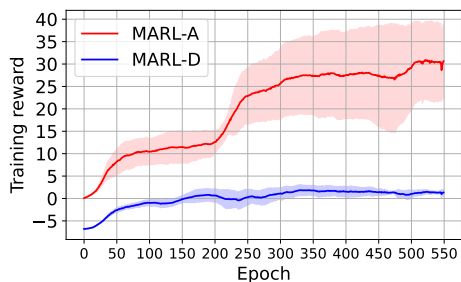
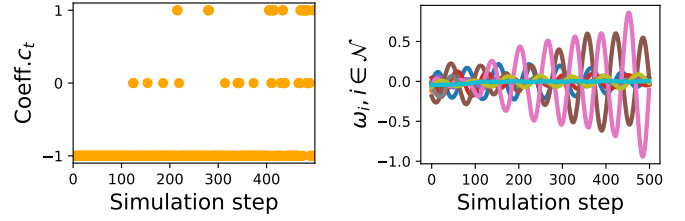


Fig. 4. History of the agent's rewards as a function of epoch. The solid line and the shaded area are the mean and standard deviation of the reward obtained with five training runs (faded color curves).

As shown in Table I, the MARL-D outperforms the offline defender against adversarial attacks in all the independent simulation runs. Despite different adversaries, the MARL-D achieves more than 60% detection accuracy. In contrast, for



(a) Droop coefficient  $c_t$  value modified by MARL-A. (b) Frequency deviation of each bus.

Fig. 5. Action of MARL-A over one episode and its physical effect.

TABLE I  
DETECTION ACCURACY (%) UNDER MARL-A'S GENERATED ATTACKS OF MULTIPLE INDEPENDENT TRAINING RUNS

$\sum_{t \in \mathcal{T}} r_t^w$	44	52	34	52	34
MARL-D	63%	65%	71%	71%	77%
Offline defender	58%	60%	36%	61%	43%

the third training run, the offline defender accuracy dropped to 36% for the MARL-A attack. This is a remarkable result since MARL-A does not have knowledge of the synthetic FDIA used to train the offline defender, and suggests that data-based FDIA defenders are vulnerable to examples that deviate from the training dataset. Figure 6 shows the attacked bus index and the identified attacked bus by the MARL-D and the offline defender. Both the offline defender and the MARL-D successfully catch the attacked bus index 6, which indicates that continuously attacking the same bus is likely to be captured. However, the MARL-D outperforms the offline defender when the adversary rapidly varies its action.

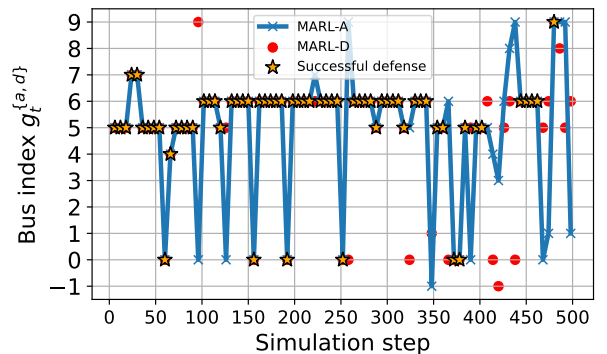


Fig. 6. Attacked bus by MARL-A and the detected bus by MARL-D. A successful defense implies  $g_t^a = g_t^d$  and the detection accuracy is 77%.

### C. Warmed-up MARL detection

In this section, we investigate whether it is reasonable to rely on an MARL training framework to construct a detection method that generalizes well to unseen attacks. These refer to FDIAs that may not be discovered by the MARL-A during the training process. For this experiment, we gauge our defender's performance against FDIAs that would cause the most system disruption, i.e., when the adversary chooses  $c_t = -1$  over the

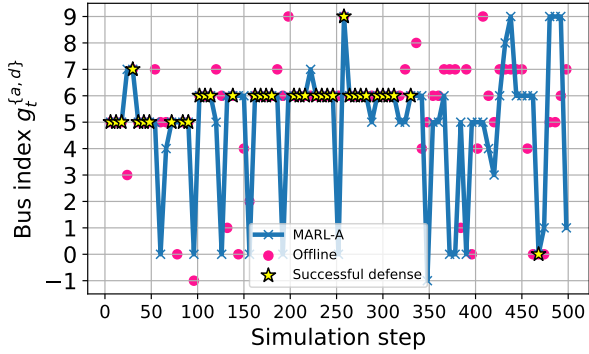


Fig. 7. The attacked bus by MARL-A and the detected bus by the offline defender. A successful defense implies  $g_t^a = g_t^d$ , and the detection accuracy is 43%.

entire control horizon (which is referred to as *time-invariant* attack) [15].

As shown in Fig. 8, the offline defender outperforms the MARL-D except for bus 6, which is often targeted by the MARL-A (Fig. 6). This shows that although MARL-A can discover a diverse set of attacks that help improve the detection performance of MARL-D, it cannot be expected to have exhaustively explored the space of FDIAs. For that reason, despite being robust to adversarial examples, MARL-D might not generalize well to FDIAs that were synthetically generated in the offline defender’s training dataset. A preferable solution is to combine the benefit of the expert knowledge available to the offline defender with the adversarial robustness of MARL-D. Here knowledge transfer can help achieve this goal. A TF-MARL-D defender is therefore trained to this end.

The performances of the TF-MARL-D are on par or even outperform (buses 2, 4, and 8) the offline defender for time-invariant attacks, which shows that the transfer learning strategy is viable to retain prior knowledge.

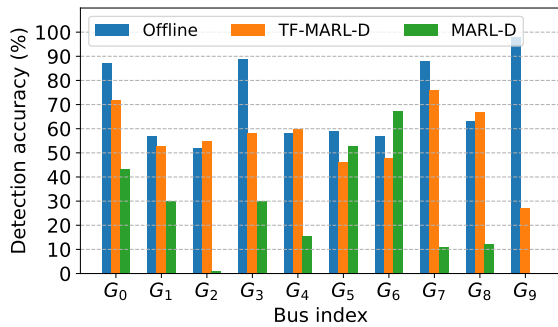


Fig. 8. The detection accuracy (%) under time-invariant attacks.

Table II shows that although the performance of TF-MARL-D is enhanced for time-invariant attacks, it still consistently outperforms the offline defender when exposed to the TF-MARL-A adversary (performance increases between 40% and 225% across 5 independent runs). Compared to MARL-A (Table I first row), the total frequency deviation induced by TF-MARL-A is reduced MARL-A. This indicates that the warm-up strategy encouraged the adversary to explore less impactful

and more stealthy FDIA.

TABLE II  
DETECTION ACCURACY (%) UNDER TF-MARL-A’S GENERATED ATTACKS OF MULTIPLE INDEPENDENT TRAINING RUNS.

$\sum_{t \in \mathcal{T}} r_t^{vd}$	20	19	21	22	18
TF-MARL-D	33%	39%	39%	42%	46%
Offline defender	22%	20%	12%	19%	33%

## V. CONCLUSION

We described and demonstrated an MARL framework that can help craft a defense strategy against stealthy and impactful FDIAs. Compared to an offline defender, the MARL defender can continuously learn to defend against newly generated adversarial FDIAs and adjust its defense strategy promptly. However, we show that MARL is not sufficient to ensure that a defender can catch all possible FDIAs. Instead, it is preferable to combine, through transfer learning, the expert knowledge from an offline defender with the MARL defender to enhance its robustness against adversarial examples.

## REFERENCES

- [1] P. Denholm, T. Mai, R. W. Kenyon *et al.*, “Inertia and the power grid: A guide without the spin,” NREL, Golden, CO, USA, Tech. Rep., 2020.
- [2] U. Tamrakar, D. Shrestha, M. Maharjan, B. P. Bhattarai, T. M. Hansen, and R. Tonkoski, “Virtual Inertia: Current Trends and Future Directions,” *Applied Sciences*, vol. 7, no. 7, 29 pages, July 2017.
- [3] Y. Li and J. Yan, “Cybersecurity of smart inverters in the smart grid,” *IEEE Trans. Power Electron.*, vol. 38, no. 2, pp. 2364–2383, 2023.
- [4] Y. Liu, P. Ning, and M. K. Reiter, “False data injection attacks against state estimation in electric power grids,” *ACM Trans. on Info. and Syst. Security*, vol. 14, no. 1, pp. 1–33, 2011.
- [5] T. Nguyen, S. Wang, M. Alhazmi *et al.*, “Electric power grid resilience to cyber adversaries,” *IEEE Access*, vol. 8, pp. 87 592–87 608, 2020.
- [6] DOE, “Electric disturbance events annual summaries,” in *Form DOE-417*, 2024. [Online]. Available: [https://www.oe.netl.doe.gov/OE417\\_annual\\_summary.aspx](https://www.oe.netl.doe.gov/OE417_annual_summary.aspx)
- [7] A. A. Habib, M. K. Hasan, A. Alkhayyat *et al.*, “False data injection attack in smart grid cyber physical system: Issues, challenges, and future direction,” *Computers and Electr. Eng.*, vol. 107, p. 108638, 2023.
- [8] A. Sahu, T. Nguyen, K. Chen *et al.*, “Detection of false data injection attacks on power dynamical systems with a state prediction method,” 2024. [Online]. Available: <https://arxiv.org/abs/2409.04609>
- [9] M. M. N. Aboelwafa, K. G. Seddik, M. H. Eldefrawy *et al.*, “A machine-learning-based technique for false data injection attacks detection in industrial iot,” *IEEE IoT J.*, vol. 7, no. 9, pp. 8462–8471, 2020.
- [10] Y. Zhang, J. Wang, and B. Chen, “Detecting false data injection attacks in smart grids: A semi-supervised deep learning approach,” *IEEE Trans. on Smart Grid*, vol. 12, no. 1, pp. 623–634, 2021.
- [11] M. R. Habibi, H. R. Baghaee, T. Dragičević *et al.*, “Detection of false data injection cyber-attacks in dc microgrids based on recurrent neural networks,” *IEEE J. Emerg. Sel. Top. Power Electron.*, vol. 9, no. 5, pp. 5294–5310, 2021.
- [12] M. Jafari, M. Ashiqur Rahman, and S. Paudyal, “Optimal false data injection attacks against power system frequency stability,” *IEEE Trans. on Smart Grid*, vol. 14, no. 2, pp. 1276–1288, 2023.
- [13] M. Choraria, A. Chattopadhyay, U. Mitra *et al.*, “Design of false data injection attack on distributed process estimation,” *IEEE Trans. on Info. Forensics and Security*, vol. 17, pp. 670–683, 2022.
- [14] J. Tian, B. Wang, J. Li, Wang *et al.*, “Exploring targeted and stealthy false data injection attacks via adversarial machine learning,” *IEEE IoT J.*, vol. 9, no. 15, pp. 14 116–14 125, 2022.
- [15] R. Prasad, M. Hassanaly, X. Zhang, and A. Sahu, “Discovery of false data injection schemes on frequency controllers with reinforcement learning,” in *2024 IEEE Power & Energy Society General Meeting (PESGM)*. IEEE, 2024, pp. 1–5.
- [16] A. S. Mohamed and D. Kundur, “On the use of reinforcement learning for attacking and defending load frequency control,” *IEEE Trans. on Smart Grid*, vol. 15, no. 3, pp. 3262–3277, 2024.

- [17] R. Huang, Y. Li, and X. Wang, "Attention-aware deep reinforcement learning for detecting false data injection attacks in smart grids," *Int. J. Electr. Power Energy Syst.*, vol. 147, p. 108815, 2023.
- [18] X. Ran, W. P. Tay, and C. Lee, "Robust data-driven adversarial false data injection attack detection method with deep q-network in power systems," *IEEE Trans. Ind. Inform.*, vol. 20, no. 8, pp. 10405–10418, 2024.
- [19] W. Cui, Y. Jiang, and B. Zhang, "Reinforcement learning for optimal primary frequency control: A lyapunov approach," *IEEE Trans. on Power Syst.*, vol. 38, no. 2, pp. 1676–1688, 2023.
- [20] P. Moritz, R. Nishihara, Wang *et al.*, "Ray: A distributed framework for emerging AI applications," in *13th USENIX symp. on operating syst. design and impl.*, 2018, pp. 561–577.